


 Cite this: *RSC Adv.*, 2021, **11**, 29939

# Highly efficient sorption of molybdenum from tungstate solution with modified D301 resin

 Fan Guo,<sup>a</sup> Xiaoli Xi,<sup>ID</sup>\*<sup>ab</sup> Liwen Ma,<sup>ac</sup> Zhuanghua Nie<sup>a</sup> and Zuoren Nie<sup>abc</sup>

The separation of molybdenum (Mo) from tungstate solution is a bottleneck problem in tungsten (W) metallurgy, and it hinders the development of high-purity tungsten materials. In this research, a modified D301 resin was used to adsorb and separate molybdenum from tungstate solution. The maximum sorption capacity ( $Q_e$ ) of modified D301 for  $\text{MoS}_4^{2-}$  was found to be  $428 \text{ mg g}^{-1}$  and the separation coefficient ( $\beta$ ) was 108.9 when the contact time was 4 h and the reaction temperature was  $25 \text{ }^\circ\text{C}$  and the pH value of the tungstate solution was 7.2. The sorption process conforms to Langmuir isotherm models and the quasi-second-order kinetic model. The sorption mechanism was also discussed, which was a single layered spontaneous sorption process. Theoretical calculations infer bonding behavior between the N atom on the resin and the S atom on the  $\text{MoS}_4^{2-}$  molecule. The sorption energy is  $-7.67 \text{ eV}$ , which indicated that the sorption process is stable chemical sorption. The desorption experiment showed that more than 90% molybdenum could be desorbed from the loaded resin when the concentration of sodium hydroxide solution was 5 w%. Finally, after three-stage sorption-desorption, almost all molybdenum in the solution was adsorbed, achieving better separation of tungsten and molybdenum.

Received 9th June 2021

Accepted 16th August 2021

DOI: 10.1039/d1ra04458c

[rsc.li/rsc-advances](http://rsc.li/rsc-advances)

## 1. Introduction

In recent years, the increasing growth of industrial waste has made the problem of environmental pollution more and more significant. Therefore, cleaner production and recycling are particularly important.<sup>1</sup> For refractory metal resources such as tungsten and molybdenum contained in waste materials, the realization of clean extraction and recycling is a hot research topic.<sup>2,3</sup> Tungsten, a national strategic resource, has a high hardness, high density, great melting point, low coefficient of thermal expansion, superb corrosion resistance, and safe processing performance, which is broadly expounded in the microelectronics, metallurgy, aerospace and other fields.<sup>4-6</sup> With the increase in tungsten consumption, the number of years of tungsten ore mining remaining is decreasing year by year, so it is necessary to recover secondary resources of tungsten. The physicochemical properties (aqueous chemical behaviors, ionic extent) of molybdenum are quite akin to those of tungsten.<sup>5,7-9</sup> So, molybdenum and tungsten easily coexist. However, the increasing needs aimed at high purity metallic tungsten and its mid product have become a severe task faced

by the metallurgical engineer.<sup>10-12</sup> Therefore, the separation of tungsten and molybdenum is an urgent problem in the recovery of tungsten secondary resources.

So far, many kinds of methods have been developed for the separation of W and Mo, such as precipitation, solvent extraction<sup>7,13</sup> and ion exchange.<sup>14-17</sup> A large amount of alkali was required to precipitate molybdenum from acidic solution to neutralize the acid in solution, which may not only introduce other impurity ions but also costs much. Solvent extraction is inconvenient in commercial production.<sup>18-20</sup> Trioctylamine (TOA) shows excellent extraction ability for Mo, and the loaded organic phase can be back-extracted with ammonium hydroxide solution. However, the separation of aqueous and organic phases is very difficult.<sup>21</sup> During the past decade, various ion exchange resins have been used for the extraction of molybdenum from solution, and the method has already been confirmed the feasibility of extracting molybdenum.<sup>22</sup> Fu *et al.* used D301 resin to directly extract  $\text{Mo(VI)}$  from the acid leaching solution of molybdenite.<sup>23</sup> D301 shows excellent sorption capacity for Mo and Mo-loaded resin can be desorbed by ammonia hydroxide solution.

The ion exchange method is one of the environmentally friendly and easy to operate secondary resource recovery methods of tungsten and molybdenum.<sup>24</sup> However, in existing literature, the sorption performance of resin on tungsten and molybdenum is almost the same. In order to develop new ion exchange resins for the separation of tungsten and molybdenum, we summarized the existing kinds of typical ion

<sup>a</sup>Collaborative Innovation Center of Capital Resource-Recycling Material Technology, Beijing University of Technology, Beijing 100124, China. E-mail: xixiaoli@bjut.edu.cn; Fax: +86-10-67391536; Tel: +86-10-67391536

<sup>b</sup>Key Laboratory of Advanced Functional Materials, Ministry of Education, Faculty of Materials and Manufacturing, Beijing University of Technology, Beijing 100124, China

<sup>c</sup>National Engineering Laboratory for Industrial Big-data Application Technology, Beijing University of Technology, Beijing 100124, China



exchange resins. Tungsten and molybdenum are mostly in the form of anions in aqueous solutions, and anion exchange resins are often used for the recovery and separation of tungsten and molybdenum. This includes strong basic D201, which is the gel-type resin, and the microporous structure will slow diffusion. The other type is weak basic D301, which has a macroporous structure, and the pore structure will facilitate diffusion. Therefore, D301 is more suitable for recovery and separation of tungsten and molybdenum in solution.

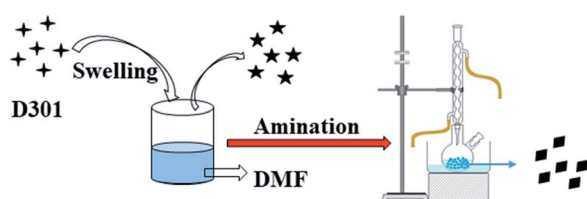
Unfortunately, the existing ion-exchange method has some disadvantages, such as difficult desorption, low sorption capacity, and weak service resistance.<sup>23,25,26</sup> Development of the new resins with high efficiency of selective sorption, desorption, and regeneration is the core of future separation technology.<sup>27,28</sup> It is reported that some resin and extractant mixtures can greatly improve the sorption capacity and the selectivity of the resin.<sup>29</sup> In addition, some heavy rare earth have been recovered with P227-impregnated resins system,<sup>17</sup> Cr(vi) have been recovered with poly-epichlorohydrin-dimethylamine (EPIDMA) modified D301 resin.<sup>30</sup>

Hence, in order to improve the sorption efficiency of D301 resin, a mixture of D301 resin and TOA was explored to separate and recovery molybdenum from tungstate solution in the present study. The sorption dynamics and sorption mechanism were investigated. According to the quantum mechanical module of Materials Studio software, the Mulliken population was calculated, and the sorption mechanism by modified D301 was obtained. Besides, optimization of sorption process conditions was studied. Furthermore, desorption experiments were conducted to study the reusability of the modified D301 resin. Finally, separation and recovery of molybdenum from tungstate solution were achieved.

## 2. Experimental section

### 2.1 Materials

D301 resin used in this study is a weakly basic anion-exchange resin with tertiary ammonium as the fixed positive charge purchased from Shanghai Kaiping Chemical Co., Ltd., China. *N,N*-Dimethylformamide (DMF, purity  $\geq 99\%$ ) and trioctylamine (TOA, purity  $\geq 95\%$ ) were kindly provided by Shanghai Macklin Biochemistry Co., Ltd. The modified D301 resin can be obtained by assembling D301 and TOA by the dipping method. The specific process is shown in Scheme 1. At first, D301 resin was washed with distilled water until reach to neutral pH value. 10 g of the D301 resin was swelled in 40 mL of DMF (purity  $\geq 99\%$ ) and aminated in 20 mL TOA at the reaction temperature of



Scheme 1 Flowcharts for the D301 resin modification reaction.

65 °C to prepare the modified D301 resin, which was prepared for the following experiments. After modification, the amination strength in modified D301 resin increases. The increase in amine content can provide more sorption sites, thereby improving the sorption performance of the resin to Mo. The stock solution included tungsten molybdenum was prepared by dissolving  $\text{Na}_2\text{WO}_3$  and  $\text{Na}_2\text{MoO}_3$  (both purity  $> 99.9\%$ ) in deionized water. All other chemicals used in this study were analytical grade.

### 2.2 Preparation of metal solutions

Three different concentrations of  $\text{Na}_2\text{WO}_4 \cdot \text{H}_2\text{O}$  solution containing molybdenum were dispensed (0.01 M W; 0.01 M Mo), (0.1 M W; 0.01 M Mo), (0.2 M W; 0.01 M Mo). Then the solution was vulcanized ( $[\text{S}]/[\text{Mo}] = 6$ ). The vulcanization process of the three kinds of solutions is the same. The pH value of the solution was pre-adjusted to 7.12 and reacted for 2.5 h at 72 °C.

### 2.3 Sorption and desorption experiments

Typically, in sorption experiments, the solid/liquid ratio was 1 g  $\text{L}^{-1}$ . 10 mg adsorbent was added to 10 mL solution with a certain concentration of  $\text{Na}_2\text{MoO}_4$ . In this study, all the sorption experiments were operated by shaking 0.02 g modified D301 with 20 mL the three different concentrations of mixed solution for 4 h. After solid-liquid separating, the aqueous phase was separated to wait for the determination of concentrations of metal elements. The effect of reaction conditions on the sorption process was studied such as reaction time, temperature and pH value. The desorption experiments were conducted by shaking the loaded modified D301 resin and 5 mL sodium hydroxide solution. And then the aqueous phase was collected. The concentration of W, Mo in the solution was tested using ICP-OES.

The removal of  $\text{MoS}_4^{2-}$  was monitored by periodically taking aliquots of the solution and determining the Mo concentration using inductively coupled plasma-atomic emission spectrometry (ICP-AES; ICP-5110, Agilent, Americana). The sorption capacity of modified D301 to  $\text{MoS}_4^{2-}$  can be expressed by  $Q_e$  (mg  $\text{g}^{-1}$ ), which was calculated as

$$Q_e = \frac{(C_0 - C_e) \times V}{m} \quad (1)$$

where  $C_0$  is the initial concentration of Mo in the solution (g  $\text{L}^{-1}$ ), and  $C_e$  is the Mo concentration after modified D301 addition (g  $\text{L}^{-1}$ ).

The separation effect of tungsten and molybdenum can be expressed by  $\beta$ , was calculated as

$$\beta = \frac{D_{\text{Mo}}}{D_{\text{W}}} \quad (2)$$

where  $D_{\text{Mo}}$  and  $D_{\text{W}}$  is the distribution ratio of molybdenum and tungsten, was calculated as

$$D = \frac{C_0 - C_e}{C_e} \quad (3)$$



## 2.4 Sorption isotherm models

The sorption isotherm process was studied based on the Langmuir and Freundlich isotherm models. These models are listed in eqn (4) and (5). In order to obtain the correlation coefficient  $R^2$  and compare the data points obtained by experiments more intuitively through the graphical, the relative parameters were calculated by nonlinear fitting.

Langmuir model:

$$\frac{C_e}{Q_e} = \frac{C_e}{Q_m} + \frac{1}{bQ_m} \quad (4)$$

Freundlich model:

$$\ln Q_e = \ln K_F + \frac{1}{n} \ln C_e \quad (5)$$

where  $C_e$  is the Mo concentration after modified D301 addition ( $\text{g L}^{-1}$ );  $Q_e$  is the maximum quantities of Mo adsorbed ( $\text{mg g}^{-1}$ );  $Q_m$  is the quantities of Mo adsorbed at equilibrium ( $\text{mg g}^{-1}$ );  $b$ ,  $K_F$  and  $n$  are the corresponding constant parameters of these models.

## 2.5 Sorption kinetics

The sorption kinetics were studied by nonlinear fitting, and two isothermal sorption models were used to fit the experimental data. These models are listed in eqn (6) and (7).

Lagergren-first-order model:

$$\ln(Q_e - Q_t) = \ln Q_e - K_1 t \quad (6)$$

Pseudo-second-order model:

$$\frac{t}{Q_t} = \frac{1}{K_2 Q_e^2} + \frac{t}{Q_e} \quad (7)$$

where  $Q_e$  is the quantities of Mo adsorbed at equilibrium ( $\text{mg g}^{-1}$ ),  $Q_t$  is the quantities of Mo adsorbed at time  $t$ , respectively ( $\text{mg g}^{-1}$ );  $K_1$  is the rate constants of Lagergren-first-order model,  $K_2$  is the rate constants of the second-order model.

## 2.6 Simulation analysis

Simulation analysis based on the density functional theory (DFT) has been widely used to explain experimental phenomena. In order to study the sorption mechanism, sorption energy and sorption configuration were calculated by Materials Studio 2020 (BIOVIA, American). The exchange correlation function of the calculation process selects the PBE function under the generalized gradient approximation (GGA).

# 3. Results and discussion

## 3.1 Preparation of materials

Firstly, the FT-IR spectra was used to illustrate the structural changes of D301 resin before and after modification. As shown in Fig. 1, a new vibration peak appears at the position of  $1667.73 \text{ cm}^{-1}$  after modification. And the vibration peak was considered as the tertiary amine functional group provided by

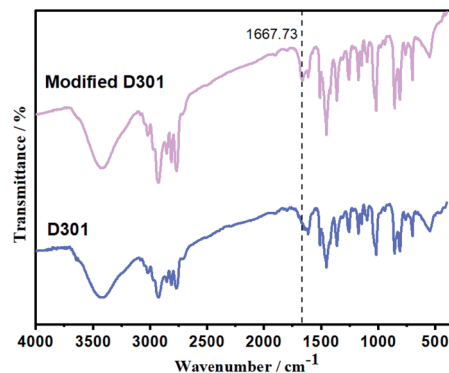


Fig. 1 FT-IR spectra of D301 resin and modified D301 resin.

the aminating agent TOA, indicating that the modified D301 resin was prepared successfully.

In the aqueous system of W-Mo-H<sub>2</sub>O, most tungsten and molybdenum are exit in the form of polymeric anions, and the two exist in very similar forms, which makes their separation difficult. However, in the W-Mo-S-H<sub>2</sub>O aqueous system, molybdenum will preferentially combine with sulfur to form Mo-S polymer ions, and W will still exist in the form of W-O anions. This makes the tungsten and molybdenum ions in the solution form an ionic difference, which increases the possibility of separation of tungsten and molybdenum ions in the solution. Therefore, in order to better separate and recover the tungsten and molybdenum solution, we first sulfide the tungsten and molybdenum solution. Fig. 2(a) showed the structures of chemical structures of NaWO<sub>4</sub>, NaMoO<sub>4</sub> and Na<sub>2</sub>S. The molar ratio of NaWO<sub>4</sub> and NaMoO<sub>4</sub> was 1 : 1, 10 : 1, 20 : 1 and all of

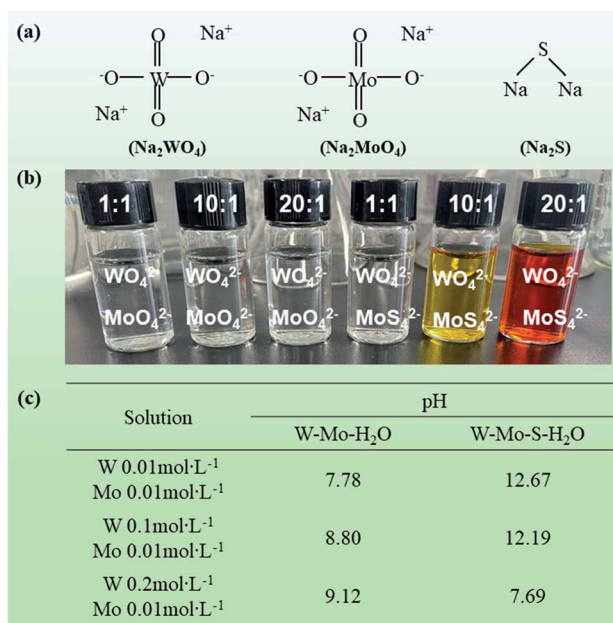


Fig. 2 (a) The molecular structure of used in this work, (b) photograph of prepared solution, (c) pH of three solutions before and after vulcanization treatment.



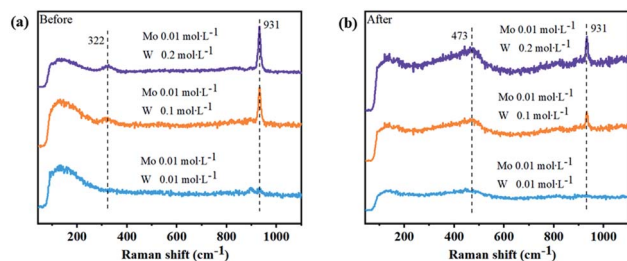


Fig. 3 Raman spectra of prepared solution (a) before and (b) after vulcanization.

the molar ratio of  $\text{NaMoO}_4$  was  $0.01 \text{ mol L}^{-1}$ . The photographs of these solution are shown in listed in Fig. 2(b). After vulcanization treatment, the colors of the solutions are obviously different.  $\text{MoO}_4^{2-}$  in the solution is colorless, and the  $\text{MoS}_4^{2-}$  in the solution is orange, combined with Fig. 2(b), we can find that, after the vulcanization treatment, the color of the solution has changed, which reflects  $\text{MoO}_4^{2-}$  in the solution was successfully converted into  $\text{MoS}_4^{2-}$  through a thiolation reaction. Among them, when the tungsten concentration is  $0.2 \text{ mol L}^{-1}$ , the solution color is lightest after vulcanization. Besides, Fig. 2(c) shows the pH changes of the three solutions before and after vulcanization treatment. It can be clearly seen that the pH of the solution is very different when the concentration of tungsten in the solution is different. As the molar ratio of tungsten increased, the pH of the solution gradually increased. The initial pH of the solution after vulcanization treatment was 12.67, 12.19 and 7.69.

In order to further confirm the combination of molybdenum and sulfur in the solution, Fig. 3 shows the Raman spectra of the solution before and after vulcanization. It can be seen from Fig. 3(a) that the Mo–O bond peak appears at  $322 \text{ cm}^{-1}$  and W–O bond appears at  $931 \text{ cm}^{-1}$  for the three solutions before vulcanization, and the peak intensity increases as the concentration of tungsten in the solution increase. After vulcanization, Mo–S bonds appear at the position of  $473 \text{ cm}^{-1}$ , but there is no W–S peak detected.

### 3.2 Sorption experiment

**3.2.1 Effect of pH value.** The main factor affecting Mo removal performance is pH value, which normally affects the characteristics of Mo in the solution.<sup>3</sup> To better improve the feasibility of practical separation processes, the species change of molybdenum and tungsten in the S–Mo–W– $\text{H}_2\text{O}$  system at pH 0–14 were investigated by thermodynamic analysis. Take the total amount of molybdenum  $c(\text{Mo}) = 0.01 \text{ mol L}^{-1}$ , the total amount of tungsten  $c(\text{W}) = 0.01\text{--}0.2 \text{ mol L}^{-1}$ , and the total amount of sulphate  $c(\text{S}) = 0.06 \text{ mol L}^{-1}$ , calculate the equilibrium concentration fraction of each ion for different pH values to examine them. The ion distribution changes with pH, and the results are shown in Fig. 4.

As shown in Fig. 4, as the pH value increases, the anions of molybdenum and tungsten change in different forms. When the pH value is more than 11, the tungsten ions in the solution

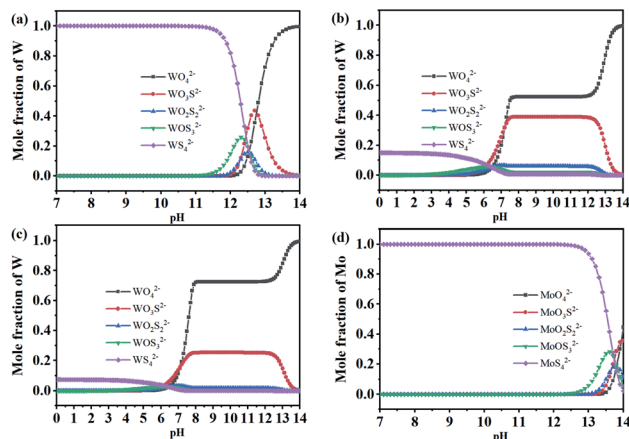


Fig. 4 The species of Mo–W–S– $\text{H}_2\text{O}$  system ( $[\text{Mo}]_{\text{T}} = 0.01 \text{ mol L}^{-1}$ ,  $[\text{S}]_{\text{T}} = 0.06 \text{ mol L}^{-1}$ ), (a) W ( $[\text{W}]_{\text{T}} = 0.01 \text{ mol L}^{-1}$ ); (b) W ( $[\text{W}]_{\text{T}} = 0.1 \text{ mol L}^{-1}$ ); (c) W ( $[\text{W}]_{\text{T}} = 0.2 \text{ mol L}^{-1}$ ); (d) Mo species.

are almost all  $\text{WO}_4^{2-}$  form exists, and in the solution of  $c(\text{W}) = 0.1 \text{ mol L}^{-1}$ ,  $c(\text{W}) = 0.2 \text{ mol L}^{-1}$ ,  $\text{WS}_4^{2-}$  in the solution is almost 0. However, Mo will combine with S to form anionic species as Mo–S compound. The distribution of  $\text{MoO}_4^{2-}$ ,  $\text{MoO}_3\text{S}^{2-}$ ,  $\text{MoO}_2\text{S}_2^{2-}$ ,  $\text{MoO}_3\text{S}^{2-}$ ,  $\text{MoS}_4^{2-}$  with the change of pH value in the solution was shown in Fig. 4(d). When the pH value is less than 12, molybdenum mainly exists in the form of  $\text{MoS}_4^{2-}$ . It is found in Fig. 4 that in the weakly alkaline or weakly acidic tungstate solution, controlling the initial pH of the solution and increasing the W concentration can make  $\text{MoO}_4^{2-}$  preferentially vulcanized, but  $\text{WO}_4^{2-}$  hardly vulcanized. The difference in the affinity of tungsten and molybdenum for sulfur can effectively separate tungsten and molybdenum. Therefore, the range of pH value 4–12 was chosen as the research range to conduct sorption optimization experiments.

The sorption performance of Mo with modified D301 at different pH values was studied at  $25^\circ\text{C}$ , the contact time is 4 h. The influence of pH values on the  $Q$  and separation factor of

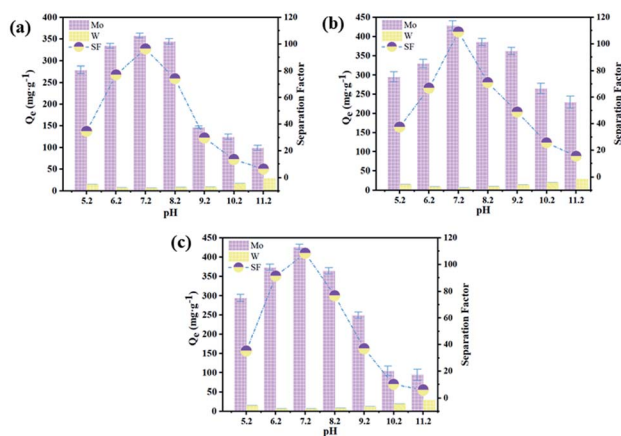


Fig. 5 Effect of different pH on  $Q_{\text{Mo}}$ ,  $Q_{\text{W}}$  and separation factor ( $[\text{Mo}]_{\text{T}} = 0.01 \text{ mol L}^{-1}$ ), (a) W ( $[\text{W}]_{\text{T}} = 0.01 \text{ mol L}^{-1}$ ); (b) W ( $[\text{W}]_{\text{T}} = 0.1 \text{ mol L}^{-1}$ ); (c) W ( $[\text{W}]_{\text{T}} = 0.2 \text{ mol L}^{-1}$ ).



modified D301 was investigated, the experimental data was shown in Fig. 5, respectively. It could be found that the calculated value of  $Q_{\text{Mo}}$  was increased firstly and then decreased with the increase of pH value. When the pH value was 7.2,  $Q_{\text{Mo}} = 428 \text{ mg g}^{-1}$ , the maximum separation factor  $\beta$  was 108.9. This is mainly because  $\text{MoO}_4^{2-}$  will release  $\text{OH}^-$  during the vulcanization process, which can be expressed as eqn (8)–(11). When increasing the pH value of the solution will also introduce  $\text{OH}^-$ , which hinders the vulcanization of  $\text{MoO}_4^{2-}$ , thereby reducing the separation factor. Then, if only the influence of  $\text{OH}^-$  is considered, the overall separation coefficient should decrease as the pH value increases. But under acidic conditions, low concentrations of  $\text{OH}^-$  may no longer be the main influencing factor. Because under acidic conditions, tungsten and molybdenum mostly exist in the form of heteropoly acid. The heteropoly acid is a macromolecular structure that will cause considerable steric hindrance, thereby reducing the sorption capacity and sorption selectivity of the resin. In summary, when the pH value is 7.2, the modified resin has the largest sorption capacity.



**3.2.2 Effect of temperature.** The molybdenum sorption capacity of modified D301 with different temperatures under sulfide solutions was tested, the results were shown in Fig. 6. As shown in Fig. 6, with an exaltation temperature from 25 °C to 75 °C, both the sorption capacity and the separation factor of modified D301 for Mo slowly decreased. It illustrated that the sorption action of Mo is an exothermic process. The temperature of 25 °C was considered the most suitable. It can also be

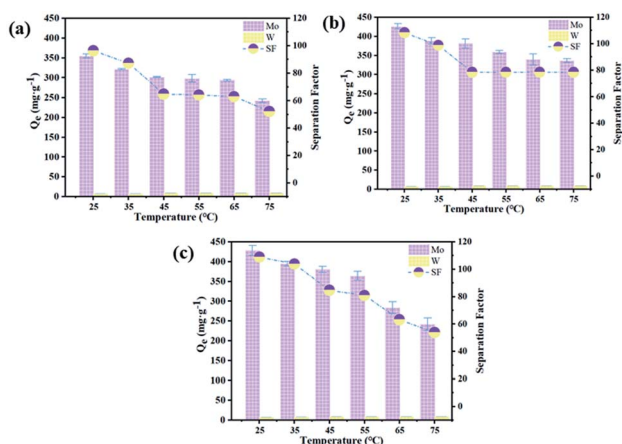


Fig. 6 Effect of different temperature on  $Q_{\text{Mo}}$ ,  $Q_{\text{W}}$  and separation factor ( $[\text{Mo}]_{\text{T}} = 0.01 \text{ mol L}^{-1}$ ), (a) W ( $[\text{W}]_{\text{T}} = 0.01 \text{ mol L}^{-1}$ ); (b) W ( $[\text{W}]_{\text{T}} = 0.1 \text{ mol L}^{-1}$ ); (c) W ( $[\text{W}]_{\text{T}} = 0.2 \text{ mol L}^{-1}$ ) at pH 7.2, 240 min.

Table 1 Comparison of the sorption capacity of some typical sorbents

Some typical sorbents	$Q_e$ ( $\text{mg g}^{-1}$ )	Ref.
TVEX-TOPO resin	17.5	33
D290 resin	76.3	34
D201 resin	85	35
Montmorillonite resin	162	36
D301 resin	157	This work
Modified D301 resin	428	This work

seen from Fig. 6, with the increase in the amount of W associated with an increase in separation factor and sorption capacity. The events explained the sorption capacity was significantly elevated with the addition of tungsten percentage in the feed solution. It is also reported in the literature that the percentage of W can influence the sorption capacity of resin, with a higher separation rate for higher W content in the solution.<sup>31</sup> Also, the amount of W can influence its sorption capacity.<sup>32</sup> Furthermore, the  $Q$  increases as the increase of the initial W concentration, for the reason that towards a certain amount of adsorbent, the higher the W percentage in the solution, the greater the concentration slope, the easier the Mo to be adsorbed.

Finally, as shown in Table 1, we summarized some typical molybdenum adsorbents.<sup>33–36</sup> Obviously, compared with other molybdenum adsorbents materials, the maximum sorption capacity ( $Q_e$ ) of modified D301 have unique advantages. The maximum sorption capacity of modified D301 for  $\text{MoS}_4^{2-}$  was found to be  $428 \text{ mg g}^{-1}$ , which is much higher than that of D301 resin. The sorption capacity increased by 2.7 times and it can greatly improve the sorption efficiency when using the same amount of resin.

### 3.3 Sorption models

Like other sorption reactions, the sorption equilibrium of modified D301 was characterized by sorption models. With the help of Langmuir model<sup>37,38</sup> and Freundlich model<sup>39</sup> the

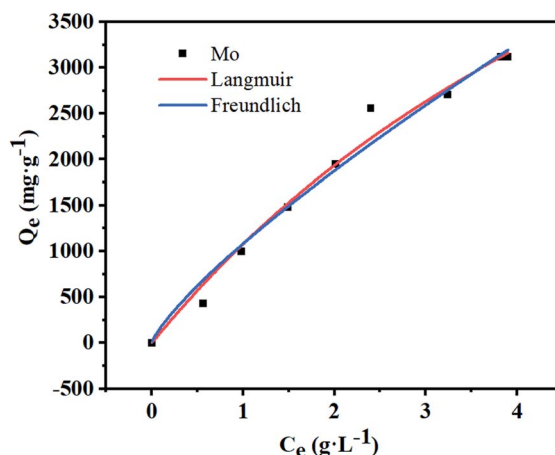


Fig. 7 Langmuir model and Freundlich model of Mo on modified D301 resin.



Table 2 The model parameters for sorption at 25 °C

Component	Equilibrium equation	$R^2$
Mo	$\frac{C_e}{Q_e} = \frac{C_e}{9440} + 0.0008$	0.987
	$\ln Q_e = 0.8 \ln C_e + 6.9$	0.971

sorption process of molybdenum by modified D301 resin was described. These two models can be expressed by eqn (4) and (5). Fig. 7 shows the sorption isotherm of molybdenum, and the correlation coefficient data is shown in Table 2. It can be seen from Fig. 7 that when the equilibrium concentration of molybdenum increases from 0 to 7.2 g L<sup>-1</sup>, and the sorption capacity can reach 2707 mg g<sup>-1</sup> at the highest. Then the correlation coefficient  $R^2$  were obtained by nonlinear fitting. The correlation coefficient  $R^2$  of the Langmuir model is 0.987 larger than that of the Freundlich model, these show that sorption progress was fitted better with the Langmuir model. So the sorption process of molybdenum is a single layered spontaneous sorption process.<sup>40</sup>

### 3.4 Sorption kinetics

To explore the sorption reaction, sorption kinetics was adopted. Kinetic behavior of Mo sorption by modified D301 was evaluated at two experiential kinetic models, the Lagergren-first-order model (eqn (6)) and the pseudo-second-order model (eqn (7)), to mathematically picture the intrinsic kinetic sorption constant.<sup>41,42</sup> To investigate the sorption kinetics of Mo with the modified D301, sorption experiments with different contact time were conducted. The sorption capacity of modified D301 was performed in Fig. 8. As shown in Fig. 8, the points in the figure represent the experimental data before nonlinear curve fitting, the solid line represents the pseudo-second-order

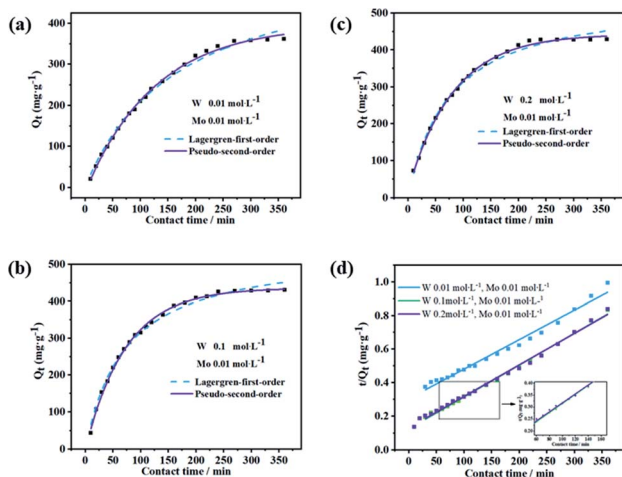


Fig. 8 Effect of different contact time on  $Q_{Mo}$  and separation factor ( $[Mo]_T = 0.01 \text{ mol L}^{-1}$ ). (a) W ( $[W]_T = 0.01 \text{ mol L}^{-1}$ ); (b) W ( $[W]_T = 0.1 \text{ mol L}^{-1}$ ); (c) W ( $[W]_T = 0.2 \text{ mol L}^{-1}$ ) at pH 7.2, 25 °C; (d) linearization of the pseudo-second-order model.

Table 3 The linear regression data of different models at 25 °C

Solution (mol L <sup>-1</sup> )	$R^2$		
	Lagergren-first-order	Pseudo-second-order	$t/Q_t - t$
W 0.01	0.992	0.998	0.983
Mo 0.01			
W 0.1	0.992	0.998	0.994
Mo 0.01			
W 0.2	0.992	0.998	0.996
Mo 0.01			

kinetic model, and the dashed line represents the Lagergren-first-order kinetic model. The  $Q$  of modified D301 to Mo increased along with the increase of operational time, suggesting a beneficial effect of the contact time on the sorption of Mo. The process reached equilibrium at about 4 h. With the accumulation of Mo, the sorption capacity increases slightly until it inclines to equilibrium, respectively. With the reaction proceeds, the molar ratio between modified D301 and Mo rise obviously, the driving force for Mo transfer decreases, therefore, a slowly increase in the sorption capacity, and then the sorption equilibrium is bit by bit reached.

The linear regression curve of different models at 25 °C is shown in Fig. 8(d). The calculated parameters are presented in Table 3.  $R^2$  figures of Lagergren-first-order kinetic model was lower than that of the pseudo-second-order kinetic model. Accordingly, the sorption kinetics were better referred to as the pseudo-second-order model, illustrating that the procedure of Mo taken up by modified D301 was chemical behavior.<sup>30</sup>

### 3.5 Sorption mechanism

In order to further clarify the sorption mechanism, a molecular model of modified D301 and  $MoS_4^{2-}$  was constructed by Materials Studio software, and the sorption reaction was simulated. As shown in Fig. 9, one  $MoS_4^{2-}$  molecular close to modified D301, and the other two move away. The S atom in  $MoS_4^{2-}$  and the N atom in the N-C bond of modified D301 are close to each other. By measuring the distance between the center radii of two atoms,  $d_1 = 168.2 \text{ pm} < r_S(1.02 \text{ pm}) + r_N(0.75$

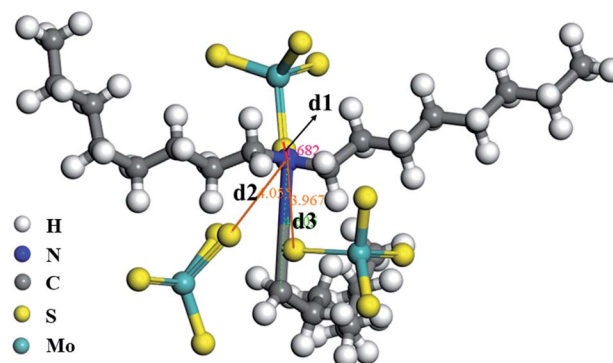


Fig. 9 The molecular models of modified D301 and  $MoS_4^{2-}$ .



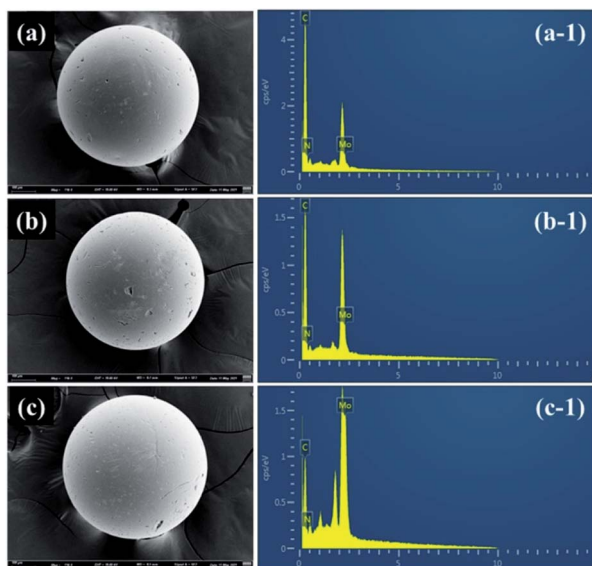


Fig. 10 SEM images and EDS analyses of adsorbed resins in (a) ( $[Mo]_T = 0.01 \text{ mol L}^{-1}$ ,  $[W]_T = 0.01 \text{ mol L}^{-1}$ ); (b) ( $[Mo]_T = 0.01 \text{ mol L}^{-1}$ ,  $[W]_T = 0.1 \text{ mol L}^{-1}$ ); (c) ( $[Mo]_T = 0.01 \text{ mol L}^{-1}$ ,  $[W]_T = 0.2 \text{ mol L}^{-1}$ ) at pH 7.2, 240 min.

pm),  $d_2 = 4.055 \text{ pm} > r_S(1.02 \text{ pm}) + r_N(0.75 \text{ pm})$ ,  $d_3 = 3.967 \text{ pm} > r_S(1.02 \text{ pm}) + r_N(0.75 \text{ pm})$ . Meanwhile, the sorption energy can get is  $-7.67 \text{ eV}$ , sorption energy is less than 0, which indicates that the sorption process is stable chemical sorption. The results of theoretical calculation can infer the bonding behavior between the N atom on the resin and the S atom on the  $MoS_4^{2-}$  molecule.

In order to understand the sorption process of Mo by modified D301 resin, Fig. 10 shows the SEM images and EDS analyses of adsorbed resins in different solutions at 240 min. It can be seen that the spherical morphology of the resin has not changed after sorption, indicating that the mechanical properties of the resin are good, which is conducive to the repeated use of the resin. In order to present the element changes after the sorption process, EDS tests were performed. EDS results demonstrate that after sorption  $MoS_4^{2-}$ , Mo in the resin is progressively appears. With the sorption proceeding, the  $MoS_4^{2-}$  ions are gradually distributed into the resin particles. When sorption action was completed, the particles were all filled with molybdenum ions, Zhao *et al.* in their study on the separation of tungsten and molybdenum obtained the content

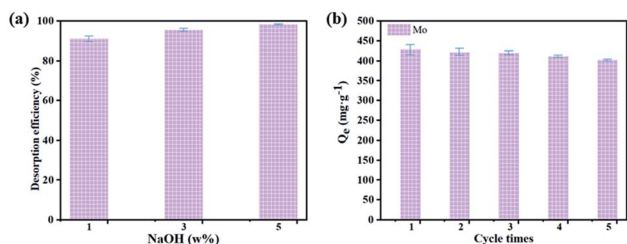


Fig. 11 (a) Desorption and (b) reusability of modified D301.

of W adsorbed in the exterior is lower than that in the interior, while for Mo, the result is the opposite.<sup>31</sup> Because Mo ions with rapid spread rate are masterly adsorbed in the internal layer, while W ions are adsorbed few in the external layer. It can also be seen from EDS that the higher the tungsten concentration in the solution, the larger the proportion of molybdenum adsorbed in the resin, which is consistent with the sorption experimental data.

### 3.6 Desorption and reusability experiments

Desorption is a necessary factor to evaluate the ion exchange system. Therefore, the desorption behavior of Mo from the loaded resin by sodium hydroxide solution was investigated, the results were shown in Fig. 11. In Fig. 11(a), different concentrations of sodium hydroxide solutions were used as eluent, and the desorption rates are all above 90%. NaOH (1–5 w%) base media was found successful reagent. Considering comprehensively, we choose 5 w% concentration of sodium hydroxide solution as the eluent. As shown in Fig. 11(b), in the 1st to 5th cycles of the sorption–desorption process, the sorption capacity of Mo with modified D301 was maintained to be high. These results indicated that the desorption capacity of sodium hydroxide solutions was high, and modified D301 could repeatedly be used for the sorption–desorption process.

### 3.7 Proposed flow sheet of separating W and Mo

On the basis of the above experimental results, a flow sheet of separating W and Mo from the tungstate solution was proposed as shown in Fig. 12. In this process, molybdate was vulcanized and separated from tungstate solution by modified D301. Moreover, modified D301 was regenerated by sodium hydroxide solutions for cycling sorption. The concentrations of three feed solution are different (0.01 M W; 0.01 M Mo), (0.1 M W; 0.01 M Mo), (0.2 M W; 0.01 M Mo). After three-stage sorption–desorption, almost all Mo in the solution can be removed. And the tungsten loss is less than 2%. The molybdenum-loaded resin was desorbed by 5 w% sodium hydroxide solution. The molybdenum in the desorption solution and tungsten in the effluent can be used as a raw material for molybdenum deep-processing products.

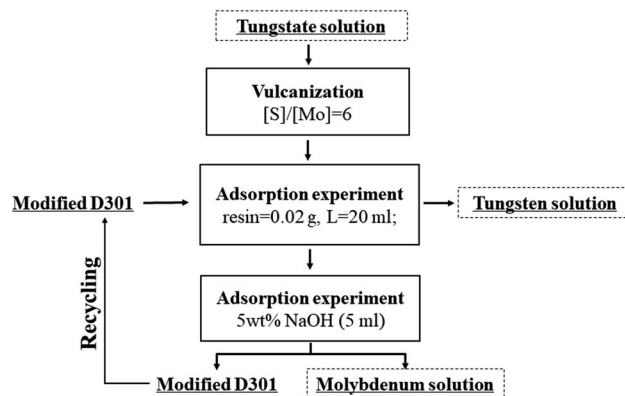


Fig. 12 Flowchart of separating W and Mo by modified D301.



## 4. Conclusions

This study proposed a sorption system of modified D301 resin, for separation and recovery of molybdenum from tungstate solution. In brief, modified D301 resin had high sorption efficiency of  $\text{MoS}_4^{2-}$  and the separation factors. In sulfur medium, when the pH value is less than 10, molybdenum mainly exists in the form of  $\text{MoS}_4^{2-}$ , tungsten mainly exists in the form of  $\text{WO}_4^{2-}$ . The maximum sorption capacity of modified D301 for  $\text{MoS}_4^{2-}$  was found to be  $428 \text{ mg g}^{-1}$  and the separation coefficient ( $\beta$ ) is 108.9 when the reaction time was 4 h and reaction temperature was  $25^\circ\text{C}$  and the pH value of tungstate solution was 7.2. The sorption process conforms to the quasi-second-order kinetic model.

The sorption mechanism was speculated by simulation analysis, the N atom in the resin and the S atom of  $\text{MoS}_4^{2-}$  can form an N-S bond during the sorption process. Besides, the desorption characteristic of  $\text{MoS}_4^{2-}$  with sodium hydroxide solution was investigated. When sodium hydroxide solution concentration was 5 w%, the desorption efficiency is 98.3%. After three-stage sorption-desorption, almost all molybdenum in the solution was adsorbed, achieving better separation of tungsten and molybdenum.

## Conflicts of interest

There are no conflicts to declare.

## Acknowledgements

This work was supported by National Key R&D Program of China (2018YFC1901700), National Natural Science Foundation of China (51621003).

## References

- 1 A. B. Cueva Sola, P. K. Parhi, J.-Y. Lee, H. N. Kang and R. K. Jyothi, Environmentally friendly approach to recover vanadium and tungsten from spent SCR catalyst leach liquors using Aliquat 336, *RSC Adv.*, 2020, **10**, 19736–19746.
- 2 Q. He and H. Chen, Increased efficiency of butanol production from spent sulfite liquor by removal of fermentation inhibitors, *J. Cleaner Prod.*, 2020, **263**, 121356.
- 3 J. Du, J. Li, D. He, M. Xu, G. Zhang, Z. Cao and S. Wu, Green separation and recovery of molybdenum from tungstate solution achieved by using a recyclable vulcanizing agent, *J. Cleaner Prod.*, 2021, **278**, 123930.
- 4 W. Jin and Y. Zhang, Sustainable Electrochemical Extraction of Metal Resources from Waste Streams: From Removal to Recovery, *ACS Sustainable Chem. Eng.*, 2020, **8**, 4693–4707.
- 5 L. Huang, M. Li, Y. Pan, Y. Shi, X. Quan and G. Li Puma, Efficient W and Mo deposition and separation with simultaneous hydrogen production in stacked bioelectrochemical systems, *Chem. Eng. J.*, 2017, **327**, 584–596.
- 6 F. Ogata, T. Nakamura, E. Ueta, E. Nagahashi, Y. Kobayashi and N. Kawasaki, Adsorption of tungsten ion with a novel Fe-

- Mg type hydrocalcite prepared at different  $\text{Mg}^{2+}/\text{Fe}^{3+}$  ratios, *J. Environ. Chem. Eng.*, 2017, **5**, 3083–3090.
- 7 H. Fu, Y. Li, G. Cao and Z. Zhao, Separation of Tungsten from Phosphorus-Containing Molybdate Solution Using Solvent Extraction with Primary Amine N1923, *Jom*, 2018, **70**(12), 2864–2868.
- 8 J. Yang, X. Chen, X. Liu, Z. Zhao, W. Wang and W. Peng, Separating W(vi) and Mo(vi) by two-step acid decomposition, *Hydrometallurgy*, 2018, **179**, 20–24.
- 9 F. Ogata, T. Nakamura and N. Kawasaki, Adsorption capability of virgin and calcined wheat bran for molybdenum present in aqueous solution and elucidating the adsorption mechanism by adsorption isotherms, kinetics, and regeneration, *J. Environ. Chem. Eng.*, 2018, **6**, 4459–4466.
- 10 W. Fu, G. Ji, H. Chen, S. Yang, B. Guo, H. Yang and Z. Huang, Molybdenum sulphide modified chelating resin for toxic metal adsorption from acid mine wastewater, *Sep. Purif. Technol.*, 2020, **251**, 117407.
- 11 D. Gong, K. Zhou, J. Li, C. Peng and W. Chen, Rapid Leaching of Synthetic Scheelite by a Resin-in-Pulp Process, *JOM*, 2018, **70**, 2846–2855.
- 12 J. Tang, Y. Liu, J. W. Ye, Z. N. Cao, S. Q. Ma and X. J. Yang, Microstructure and mechanical properties improvements in cemented carbides by (Cr,Mo,Ta)<sub>2</sub>(C,N) inhibitors, *Rare Met.*, 2020, 679–686.
- 13 T. H. Nguyen and M. S. Lee, Separation of molybdenum(vi) and tungsten(vi) from sulfate solutions by solvent extraction with LIX 63 and PC 88A, *Hydrometallurgy*, 2015, **155**, 51–55.
- 14 M. F. Hamza, K. A. M. Salih, A. A. H. Abdel-Rahman, Y. E. Zayed, Y. Wei, J. Liang and E. Guibal, Sulfonic-functionalized algal/PEI beads for scandium, cerium and holmium sorption from aqueous solutions (synthetic and industrial samples), *Chem. Eng. J.*, 2021, **403**, 126399.
- 15 F. Liu, R. Hua, F. Zhang, H. Liu, C.-P. Lee, H. Liu and B. Xu, Adsorption and separation of Re(vii) using trimethylamine-functionalized strong base anion exchange resin, *J. Radioanal. Nucl. Chem.*, 2020, **326**, 445–454.
- 16 W. Wang, A. Maimaiti, H. Shi, R. Wu, R. Wang, Z. Li, D. Qi, G. Yu and S. Deng, Adsorption behavior and mechanism of emerging perfluoro-2-propoxypropanoic acid (GenX) on activated carbons and resins, *Chem. Eng. J.*, 2019, **364**, 132–138.
- 17 B. Yang, S. Wu, X. Liu, Z. Yan, Y. Liu, Q. Li, F. Yu and J. Wang, Solid-phase extraction and separation of heavy rare earths from chloride media using P227-impregnated resins, *Rare Met.*, 2020, **40**, 2633–2644.
- 18 Y. Song, Y. Tsuchida, M. Matsumiya, Y. Uchino and I. Yanagi, Separation of tungsten and cobalt from WC-Co hard metal wastes using ion-exchange and solvent extraction with ionic liquid, *Miner. Eng.*, 2018, **128**, 224–229.
- 19 S. Van Roosendael, M. Regadio, J. Roosen and K. Binnemans, Selective recovery of indium from iron-rich solutions using an Aliquat 336 iodide supported ionic liquid phase (SILP), *Sep. Purif. Technol.*, 2019, **212**, 843–853.





- 20 X. Wu, G. Zhang, L. Zeng, W. Guan, S. Wu, Z. Li, Q. Zhou, D. Zhang, J. Qing, Y. Long, J. Li, Q. Li, Z. Cao and L. Xiao, Continuous solvent extraction operations for the removal of molybdenum from ammonium tungstate solution with quaternary ammonium salt extractant, *Hydrometallurgy*, 2020, **195**, 105401.
- 21 M. Ghadiri, S. N. Ashrafzadeh and M. Taghizadeh, Study of molybdenum extraction by trioctylamine and tributylphosphate and stripping by ammonium solutions, *Hydrometallurgy*, 2014, **144**, 151–155.
- 22 A. Daud, G. Gray, C. D. Lynch, N. H. F. Wilson and I. R. Blum, A randomised controlled study on the use of finishing and polishing systems on different resin composites using 3D contact optical profilometry and scanning electron microscopy, *J. Dent.*, 2018, **71**, 25–30.
- 23 Y. Fu, Q. Xiao, Y. Gao, P. Ning, H. Xu and Y. Zhang, Direct extraction of Mo(vi) from acidic leach solution of molybdenite ore by ion exchange resin: Batch and column adsorption studies, *Trans. Nonferrous Met. Soc. China*, 2018, **28**, 1660–1669.
- 24 H. MacKeown, J. A. Gyamfi, M. Delaporte, K. V. K. M. Schoutteten, L. Verdickt, B. Ouddane and J. Criquet, Removal of disinfection by-product precursors by ion exchange resins, *J. Environ. Chem. Eng.*, 2021, **9**, 20–24.
- 25 Y. Cao, Q. Guo, Z. Shu, C. Jiao, L. Luo, W. Guo, Q. Zhao and Z. Yin, Tungstate removal from aqueous solution by nanocrystalline iowaite: An iron-bearing layered double hydroxide, *Environ. Pollut.*, 2019, **247**, 118–127.
- 26 N. Reynier, L. Coudert, J. F. Blais, G. Mercier and S. Besner, Treatment of contaminated soil leachate by precipitation, adsorption and ion exchange, *J. Environ. Chem. Eng.*, 2015, **3**, 977–985.
- 27 R. Li, N. Liang, X. Ma, B. Chen and F. Huang, Study on the adsorption behavior of glycerin from fatty acid methyl esters by a tertiary amine-type anion exchange resin, *J. Chromatogr. A*, 2019, **1586**, 62–71.
- 28 R. V. Xikhongelo, F. M. Mtunzi, P. N. Diagboya, B. I. Olu-Owolabi and R.-A. Düring, Polyamidoamine-Functionalized Graphene Oxide-SBA-15 Mesoporous Composite: Adsorbent for Aqueous Arsenite, Cadmium, Ciprofloxacin, Ivermectin, and Tetracycline, *Ind. Eng. Chem. Res.*, 2021, **60**, 3957–3968.
- 29 F. Q. An, Y. Wang, X.-Y. Xue, T.-P. Hu, J.-F. Gao and B.-J. Gao, Design and application of thiourea modified D301 resin for the effective removal of toxic heavy metal ions, *Chem. Eng. Res. Des.*, 2018, **130**, 78–86.
- 30 Y. Zang, Q. Yue, Y. Kan, L. Zhang and B. Gao, Research on adsorption of Cr(vi) by Poly-epichlorohydrin-dimethylamine (EPIDMA) modified weakly basic anion exchange resin D301, *Ecotoxicol. Environ. Saf.*, 2018, **161**, 467–473.
- 31 Z. Zhao, J. Zhang, X. Chen, X. Liu, J. Li and W. Zhang, Separation of tungsten and molybdenum using macroporous resin: Equilibrium adsorption for single and binary systems, *Hydrometallurgy*, 2013, **140**, 120–127.
- 32 X. z. Zhu, G. s. Huo, J. Ni and Q. Song, Removal of tungsten and vanadium from molybdate solutions using ion exchange resin, *Trans. Nonferrous Met. Soc. China*, 2017, **27**, 2727–2732.
- 33 B. A. Masry and J. A. Daoud, Sorption behavior of tungsten and molybdenum on TVEX-TOPO resin from nitric acid solution, *J. Chem. Technol. Biotechnol.*, 2021, 1399–1410.
- 34 L. S. Xiao, Q. X. Zhang, B. F. Gong and S. Y. Huang, Separation of molybdenum from tungstate solution by a combination of moving packed bed and fluid bed ion-exchange techniques, *Int. J. Refract. Met. Hard Mater.*, 2001, **19**, 145–148.
- 35 Z. Zheng, Q. Jia, X. Xie, X. Zheng, C. Yao, C. Xiong and J. Jiang, Removal and Recovery of Mo(IV) from Aqueous Solutions by D201 Resin: Adsorption and Column Studies, *Asian J. Chem.*, 2014, **26**, 393–395.
- 36 M. Tuchowska, B. Muir, M. Kowalik, R. P. Socha and T. Bajda, Sorption of Molybdates and Tungstates on Functionalized Montmorillonites: Structural and Textural Features, *Materials*, 2019, **12**, 2253.
- 37 I. Langmuir, The constitution and fundamental properties of solids and liquids, *J. Am. Chem. Soc.*, 1916, **38**, 2221–2295.
- 38 X. Chen, Z. Tian, H. Cheng, G. Xu and H. Zhou, Adsorption process and mechanism of heavy metal ions by different components of cells, using yeast (*Pichia pastoris*) and Cu<sup>2+</sup> as biosorption models, *RSC Adv.*, 2021, **11**, 17080–17091.
- 39 A. W. Adamson and A. P. Gast, *Physical chemistry of surfaces*, Interscience Publishers New York, 1967, vol. 150.
- 40 S. Hassanpour and M. Taghizadeh, Rapid and selective separation of molybdenum ions using a novel magnetic Mo(vi) ion imprinted polymer: a study of the adsorption properties, *RSC Adv.*, 2016, **6**, 100248–100261.
- 41 J. P. Simonin, On the comparison of pseudo-first order and pseudo-second order rate laws in the modeling of adsorption kinetics, *Chem. Eng. J.*, 2016, **300**, 254–263.
- 42 I. A. Tan, A. L. Ahmad and B. H. Hameed, Adsorption of basic dye on high-surface-area activated carbon prepared from coconut husk: equilibrium, kinetic and thermodynamic studies, *J. Hazard. Mater.*, 2008, **154**, 337–346.

